

Article

Alkali-Activated Binder Based on Cupola Dust of Mineral Wool Production with Mechanical Activation

Pavel Fedorov *  and Dmitry Sinitsin

Department of Building Structures, Institute of Architecture and Construction,
Ufa State Petroleum Technological University, 450064 Ufa, Russia

* Correspondence: fpa_idpo@mail.ru; Tel.: +7-347-228-22-00

Abstract: The development of low-carbon alkali-activated binders based on production waste is one of the most sought-after areas of development of building materials science. The article examines the results of studies of the structures of cupola dust and the assessment of its ability to hydrate when exposed to alkaline activation. Technological preparation of dust by sifting it through a 0.16 mm sieve and subsequent mechanical activation for 120 s to a specific surface area of 733 m²/kg is proposed. The best results were shown by the composition of cupola dust with an alkaline activator of 50 wt.% 8.3 M NaOH and 50 wt.% Na₂SiO₃. After 28 days of natural hardening for this composition, the bending strength was 12.7 MPa and the compressive strength was 68.3 MPa. The analysis of the influence of hardening conditions showed that the temperature–humidity treatment of concrete at a temperature of 90 °C for 12 h accelerates the process of curing to 80–90% of natural conditions. The porosity of the samples after heating was established, which is 24–25%. The mineralogical composition of the products of the cement matrix structure’s formation, which is represented by minerals of the zeolite group, was specified.

Keywords: alkali-activated binder; waste of mineral wool production; cupola dust; fineness of grinding; strength; porosity; mineral composition



Citation: Fedorov, P.; Sinitsin, D. Alkali-Activated Binder Based on Cupola Dust of Mineral Wool Production with Mechanical Activation. *Buildings* **2022**, *12*, 1565. <https://doi.org/10.3390/buildings12101565>

Academic Editor:
Francesco Colangelo

Received: 23 August 2022

Accepted: 27 September 2022

Published: 29 September 2022

Publisher’s Note: MDPI stays neutral with regard to jurisdictional claims in published maps and institutional affiliations.



Copyright: © 2022 by the authors. Licensee MDPI, Basel, Switzerland. This article is an open access article distributed under the terms and conditions of the Creative Commons Attribution (CC BY) license (<https://creativecommons.org/licenses/by/4.0/>).

1. Introduction

The world is implementing the UN plan [1] to achieve a better and more sustainable development of mankind, consisting of 17 goals such as combating climate change, responsible consumption and production, and so on. There are a number of global problems that hinder the implementation of this plan. Such problems include an increase in greenhouse gases, primarily CO₂ emissions, depletion of natural resources and the formation of multi-ton waste as a result of economic activity. Portland cement is one of the main industries contributing to the escalation of these problems [2]. In turn, Portland cement is the main binder for concrete and reinforced concrete in the production of products and structures for industrial, civil and transport purposes. It is currently not possible to opt out of using it. Moreover, its production volume is constantly increasing. Thus, according to M. Garside [3], in 1995, cement production in the world amounted to 1.39 billion tons, and in 2021 it amounted to 4.4 billion tons. The largest cement production is in China [4]. In 2020, 2.4 billion tons of cement were produced on its territory [4,5]. Russia is one of the 20 largest cement producing countries. In 2020, 51.7 million tons were produced in Russia [6]. According to IEA [7] forecasts for 2050, cement production in the world will amount to 4.68 billion tons. In turn, the forecast for CO₂ emissions up to 2050 in the cement industry distinguishes two scenarios [8]. In the first scenario, emissions are stabilized at the level of 2400 CO₂ emissions Mt/year; in the second scenario, there is an increase in emissions—over 2700 CO₂ emissions Mt/year. In the future, the general trend in cement production tends to fade. Perhaps this is due to the increase in the use of “green” technologies based on wood and plastics or other factors. In any case, at the current rate of

Portland cement use and public disregard for the carbon footprint of the materials, this will lead to a further increase in greenhouse gas emissions in the cement industry. With more stringent carbon regulation, further technological innovations and increasing the value of green concrete and other sustainable environmentally friendly solutions, this process can be slowed down or minimized.

One solution to this problem is the development of low carbon binders based on an alkaline reaction. Low-carbon binders not only reduce CO₂ emissions but are also more environmentally friendly than Portland cement, as they allow the use of industrial by-products as feedstock, which emit less of this gas.

Based on the above, concretes based on slag-alkali binders are of scientific interest, which is confirmed by the conclusions and forecasts of the technical committee RILEM TC 224-AAM [9]. However, due to the constant demand for finely ground granulated blast-furnace slag, used as an additive to reduce clinker in Portland cement and separately constituting the main component of the alkaline binder, this leads to an increase in its cost. Therefore, the search for alternative components remains a topical issue.

International experience shows that when developing low-carbon binders, two groups of studies are distinguished:

- development of complex structured composite cements with a decrease in the content of clinker and an increase in the content of additives of natural and technogenic origin in them [10–14];
- development of the production of clinker-free binders, alternative in properties to Portland cement [15–19].

The first group includes traditional binders, which include cement clinker. The cements of this group are generally classified into five types of cement with mineral additives. These cements with mineral additives are primarily characterized by the replacement of a part of Portland cement with active or inert mineral additives (blast furnace slag, fly ash, etc.) with an inevitable decrease in binder activity and, consequently, subsequent performance properties [20–22]. Thus, according to Alekseev S.N. and Rosenthal N.K. [21], for cement with the addition of blast-furnace slag, the carbonization rate is higher than that of ordinary Portland cement. Basically, these cements are low-quality binders. The peculiarity of such cements is a long curing and low resistance in various industrial environments. Currently, a number of researchers [23,24] are focusing on improving the performance properties by optimizing the technological properties of cement or concrete mixture, namely, reducing the consumption of cement in concrete, using chemical additives, mineral additives, optimizing aggregates, etc.

The second group includes slag-alkaline, alkaline binders obtained on the basis of finely dispersed aluminosilicates of natural and technogenic origin by mixing them with aqueous solutions of alkalis and, in this case, forming low-basic hydrosilicates of calcium, silicic acid, alkaline and alkaline–earth hydroaluminosilicates, hydroaluminates and hydroferrites [16].

These binders are obtained using alkaline activation, by-products of granulated blast-furnace and cupola slags, fly ash and bottom ash, metakaolinite and others [25]. As a result, the use of Portland cement (namely clinker) is excluded and, at a higher level, carbon dependence is reduced and the environment is improved due to resource saving.

Of the variety of low-carbon binders, the most studied in terms of properties, composition, structure and durability are Portland cements with the addition of mineral additives of the “CEM I ... V” types, that is, binders of the first group. In turn, according to Eroshkina N.A. and Korovkina M.O. [26], there is a difficulty in studying the mechanism of the hardening of binders of the second direction, since there is a large scatter of the obtained experimental data due to the variability of the compositions of raw materials from by-products of processing.

One of the promising wastes for low-carbon binders is cupola dust from mineral wool production. This dust is formed during the purification of waste gases from the cupola furnace of mineral wool production [27–29]. Unlike other waste from this industry, there is

no cost-effective recycling or reuse program for cupola dust that could significantly reduce its accumulation [30].

Kubiliute R. et al. [31] proposed to use cupola dust as an additive to Portland cement, and it was also found that its addition helps to increase the compressive strength of the cement stone and accelerate the hydration of calcium silicates. The authors recommend washing the dust to reduce the chlorides in it.

According to Nagrockiene D. [32], for clinker cements modified with dust from mineral wool production waste in the amount of 5% by weight of cement weight, the compressive strength increases by 8.3% relative to concrete without additives. With an increase in the content to 7.5% of the cement weight, a decrease in compressive strength is observed up to 2.7% higher than the value in relation to concrete without additives. With a dust content of 7.5% by weight of cement, the samples absorb less water due to low porosity, which increases frost resistance. In the study [30], it was shown that when developing compositions of refractory concrete based on calcium aluminate cement, cupola dust could act as a substitute for technical microsilica. Belov V.V. and others [33] write that in the compositions of fine-grained concrete using complex waste of mineral wool production, namely in the optimal composition consisting of 1% of the volume of concrete of fibrous basalt waste, 10% of the mass of cement of dust-like waste, compared with the composition without the additive the compressive strength, increases by 11.5 MPa for cube samples and by 5.3 MPa for prism samples; the increase in tensile strength in bending of the prism samples is 1.87 MPa.

In slag-alkali binders and geopolymers, as a rule, it is proposed to use either wastes consisting of mineral elements (beads, slags, dust) formed at different stages [17] or mineral wool as a recycling process [34].

Erofeev V. et al. [17] found that the process of structure formation in the system “Mineral wool production waste–Water–NaOH” is most effective at a NaOH/waste ratio of 2/100–3/100. The best indicators of the physical and mechanical properties of the obtained binders are achieved with a waste grinding fineness equal to 400–450 m²/kg. The compressive strength of the developed binder compositions reaches 68 MPa, and, in bending, at a waste grinding fineness of 300 m²/kg, it is already 13.5 MPa. They also showed that composites based on binders from mineral wool production waste are water-resistant and fungus-resistant, and some compositions are fungicidal.

Kinnunen P. et al. [34] have developed a geopolymer consisting of 33% fibre mineral wool waste and 47% fly ash with a water-binding ratio of 0.4 and a SiO₂/Al₂O₃ ratio of 2.47. The compressive strength of this geopolymer is over 12 MPa.

According to Puertas F. and Torres-Carrasco M. [35], in slag-alkali binders with the addition of glass waste, as a result of treatment with alkaline activators from NaOH and liquid glass, blast-furnace slag was activated and, while partially dissolving it, compounds and a microstructure, observed in a slag-alkali binder based on liquid glass, were formed.

Davidovits J. [16] indicates that hydration products in geopolymers are formed as a result of the interaction of calcium hydrosilicates and sodium hydroaluminosilicates. In the presence of clay minerals in the binder when they interact with alkalis, hydroaluminosilicates (zeolites) are synthesized,

The mechanism is more complex in geopolymers due to the high content of CaO, so a number of studies have been carried out to study its role in the polymerization process [36,37]. It was found that CaO positively affects the strength of geopolymer bonds and plays an important role in determining the reaction path and the physical properties of the products of the hydration process. Moreover, the formation of CaO compounds has been reported to be highly dependent on the SiO₂/Al₂O₃ ratio and the pH value.

From most alkaline activators, NaOH, Na₂SiO₃, Na₂CO₃, Na₂O·nSiO₂ and Na₂SO₄ are common [38–40]. Some potassium compounds (potassium hydroxide) were used in some studies. However, experience with their use is limited due to economic performance. According to Sajedi F. and Razak H.A. [40], the properties of alkaline binders based on sodium and potassium compounds are very similar.

Rusina V.V. [18] notes the expediency of using liquid glass from microsilica in the production of clinker-free binders. The strength of the samples obtained as a result of temperature–humidity processing of the test of normal density of samples of different compositions using fly ash, slag binder and liquid glass from microsilica is 21.7–92.8 MPa, and the softening coefficient in all cases exceeds 0.8. The results of fine analysis methods showed that in such samples the composition of the hydrated phases does not differ from the products of known alkaline and slag-alkali binders.

Palomo A. et al. [41] found that various fly ash specimens activated with 8–12 M NaOH cured at 85 °C for 24 h produced specimens with compressive strengths ranging from 35 to 40 MPa. In addition, the strength can reach almost 90 MPa if a water glass is added to NaOH ($\text{SiO}_2/\text{Na}_2\text{O} = 1.23$).

According to Ruengsillapanun K. et al. [42], while using fly ash with a high calcium content as a binder and alkaline activator from Na_2SiO_3 and NaOH solution with concentrations of 2, 4, 6 and 8 M with an increase in the $\text{Na}_2\text{SiO}_3/\text{NaOH}$ ratio and NaOH concentration, the compressive strength of concrete increases. Therefore, at a ratio of 0.5 and a concentration of NaOH 2 M solution after 90 days, the compressive strength is 27.5 MPa. Shrinkage tends to decrease at higher NaOH solution concentrations and increase at higher $\text{Na}_2\text{SiO}_3/\text{NaOH}$ ratios. The heat release of concrete with alkali-activated fly ash is two times lower than that of concrete made from ordinary Portland cement at the same compressive strength. Increasing the NaOH concentration and the $\text{Na}_2\text{SiO}_3/\text{NaOH}$ ratio resulted in a higher temperature rise of the alkali-activated concrete.

Production waste, as a rule, has a smaller specific surface than the binder, so preparatory work is required to change the particle size distribution. An increase in the fineness of the grinding of binder particles leads to an increase in their surface area, which contributes to an increase in the degree of packing of the cement matrix [43]. According to the data of work [44], when using mechanical activation of industrial wastes used in the compositions of binder cement mortars, an increase in cement strength is observed (up to 40%).

For alkali-activated binders, the hardening conditions and the period of strength development of the alkali-activated binder play an important role in strength. A comparative analysis by Castillo et al. [45] showed that higher temperatures and holding times promote intense N-A-S-H gel formation, which leads to an increase in mechanical characteristics. The greatest strength can be achieved at a temperature of 80–90 °C [45,46].

Traditionally, the total period of curing in the natural hardening chamber for clinker and non-clinker cements is 28 days. However, hydration processes continue after this time. Thus, according to the data of works [43,47], there is a slight increase in the strength of alkaline concretes and mortars in 60 and 90 days. However, the main set of strength occurs within 28 days.

The durability of alkali-activated concretes remains a debatable issue due the large scatter of data caused by the use of different raw materials. Wang A. et al. [48], after reviewing the work on the durability of concretes from alkali-activated binders and Portland cement, found that, in general, alkali-activated concretes have a greater durability than those from Portland cement. At the same time, three groups of binders are distinguished, differing in the mechanism of concrete corrosion in different working environments: without CaO content, low in CaO and high in CaO. For example, in work [49], slag-alkali concrete was prepared. It was based on granulated blast-furnace slag activated with a high-concentration alkali solution; during hardening, it was found that this concrete, in a short time, reached a strength comparable to concrete on Portland cement. However, the material showed an increase in the number of voids, as well as a decrease in speed over time. This can cause the material to perform worse for longer periods of time. This is due to the fact that a large amount of CaO is present in the blast-furnace slag, so the corrosion mechanism will obviously be similar to Portland cement, which is confirmed by the conclusions given in [48]. According to [48], one of the proposals to increase the durability of alkali-activated concrete is to reduce the porosity of the structure through the use of nano- SiO_2 .

Based on the foregoing, it can be concluded that the development of compositions of low-carbon binders based on production by-products, including cupola dust as raw materials and their subsequent activation with metal alkalis, is an urgent task that contributes to the resource saving of materials and the reduction in greenhouse gases.

The main purpose of this study is to develop compositions based on cupola dust of mineral wool production with mechanical activation, as the main raw material for the production of alkali-activated binder. This paper presents the results of original studies of the analysis of the structure of cupola dust in terms of chemical, mineralogical and granulometric compositions and assessment of the influence of the fineness of grinding cupola dust on the physical, mechanical and technological properties of the alkali-activated binder. The results of the selection of compositions with different activators, such as NaOH, KOH and NaOH+Na₂SiO₃, are described. A comparative analysis of the influence of natural and accelerated conditions of concrete hardening on strength indicators has been made. The structure and products of the cement matrix of the obtained concretes were studied.

2. Materials and Methods

To achieve this goal, the following tasks were performed:

- study of the structure of cupola dust,
- assessment of the effect of technological parameters on the properties of alkali-activated binders from cupola dust,
- study of the structure and products of neoplasms of the cement matrix.

As the main component of the binder, cupola dust was taken, which is formed during the purification of cupola gases in the production of mineral wool boards by Agidel LLC (Blagoveshchensk, Republic of Bashkortostan, Russia). Dust is a mixture of grey colour, including fine fractions and large inclusions up to 10 mm. Since the main components for the production of mineral wool are rocks of the basalt group of the Abzakovo deposit (Republic of Bashkortostan, Russia), as well as foundry coke, blast-furnace slag, porphyrite, etc.; obviously, the mineral dust of these components is present in cupola dust.

A general view of cupola dust is shown in Figure 1.



Figure 1. General view of cupola dust.

An alkaline activator was adopted in three types: sodium hydroxide solution NaOH, a solution of caustic potassium KOH and a 50 wt.% solution of sodium hydroxide NaOH and 50 wt.% sodium metasilicate Na₂SiO₃.

The study used technical caustic soda flake produced by JSC Bashkir Soda Company (Sterlitamak, Russia) and caustic potash produced by UNID Co, Ltd. (Ulsan, Republic of Korea).

Drinking water, according to GOST 23732–2011 [50], was used to prepare alkali solutions. The concentration of solutions of 8.3 M was taken as the working concentration of NaOH and KOH. The required density of the NaOH solution at a temperature of 20 °C was taken as 1.2840 g/mL and, for the KOH solution, 1.3282 g/mL. Density control was carried out using an AON-1 hydrometer.

As an additional activator, sodium metasilicate Na₂SiO₃ of the Universal brand produced by Teks LLC (Russia) was used. It was a yellow liquid. The density of the solution at a temperature of 20 °C was 1.36 kg/L.

For the manufacture of “reference” control samples for the study, Portland cement of the brand CEM I 42.5N produced by Magnitogorsk Cement and Refractory Plant LLC (Magnitogorsk, Russia) was taken. The chemical composition of Portland cement is shown in Table 1.

Table 1. Chemical composition of Portland cement.

Fe ₂ O ₃ + FeO	Al ₂ O ₃	SiO ₂	CaO	Na ₂ O	SO ₃	MgO	Loss on Ignition
4.27	5.24	20.80	60.45	0.61	2.81	4.02	1.60

As a fine aggregate, polyfractional quartz sand, composed of quarry sand (Kabakovo village, Republic of Bashkortostan, Russia) in accordance with the granulometric composition GOST 30744-2001 [51], was used.

The granulometric composition of polyfractional sand is shown in Table 2.

Table 2. The particle size distribution of polyfractional sand.

Name of Balance	Bottom	Particle Size, mm					
		0.08	0.16	0.5	1.00	1.25	2.0
Residue on sieve, g	–	36	580	230	47	107	–
Private balance, %	–	3.6	58.0	23.0	4.7	10.7	–
Total balance, %	–	100	96.4	38.4	15.4	10.7	–

The content of dust and clay particles in the sand was about 1.8%; therefore, the sand was additionally washed and dried before the start of the research. The true density of the sand was 2.97 g/cm³.

The following types of binder compositions were used in the study: C1—reference composition—Portland cement; C2—cupola dust after screening through a 0.16 mm sieve, alkaline activator NaOH 8.3 M; C3—cupola dust after screening through a 0.16 mm sieve and mechanical activation for 60 s in a ball mill, alkaline activator NaOH 8.3 M; C4—cupola dust after screening through a 0.16 mm sieve and mechanical activation for 120 s, alkaline activator NaOH 8.3 M; C5—cupola dust after screening through a 0.16 mm sieve and alkaline activation for 240 s, alkaline activator NaOH 8.3 M; C6—cupola dust after screening through a 0.16 mm sieve and mechanical activation for 120 s, alkaline activator composition 50 wt.%, NaOH solution 8.3 M and 50 wt.% Na₂SiO₃; C7—cupola dust after screening through a 0.16 mm sieve and alkaline activation for 120 s, alkaline activator KOH 8.3 M.

The determination of strength characteristics was carried out on samples from a cement–sand mortar with a composition of 1:3. The consumption of components is shown in Table 3.

Table 3. Consumption of raw materials for the preparation of cement–sand mortar test samples.

Type of Composition	Composition Number	Binding Agent (B), kg/m ³		Water, kg/m ³	Alkaline Activator, kg/m ³			W/B ¹	Sand, kg/m ³
		Portland Cement	Cupola Dust		Lye in Dry State		Sodium Silicate Na ₂ SiO ₃		
					NaOH	KOH			
C1	C1a, C1b	450	–	189	–	–	–	0.42	1350
C2	C2a, C2b	–	450	214	75	–	–	0.41	1350
C3	C3a, C3b	–	450	214	75	–	–	0.41	1350
C4	C4a, C4b	–	450	214	75	–	–	0.41	1350
C5	C5a, C5b	–	450	214	75	–	–	0.41	1350
C6	C6a, C6b	–	450	107	37	–	153	0.53 ²	1350
C7	C7a, C7b	–	450	241	–	130	–	0.42	1350

¹ The amount of binder is taken as the sum of cupola dust and alkali in a dry state. ² To determine W/B, the amount of water was taken, taking into account Na₂SiO₃, in the amount of 112.5 kg/m³.

Compositions of type C2, C3, C4 and C5 were used to study the effect of mechanical activation of cupola dust on strength; compositions of type C1, C4, C6 and C7 were used to compare different alkaline activators. Samples with composition numbers C1a, C2a, C3a, C4a, C5a, C6a and C7a were kept in a natural hardening chamber for 28 days; samples with composition numbers C1b, C2b, C3b, C4b, C5b, C6b and C7b were subjected to temperature and humidity treatment.

The mode of temperature–humidity treatment of the samples was adopted as one-stage isothermal heating with a duration of 3 + 6 + 3 = 12 h. Samples were heated to a temperature of 90 °C.

A common parameter for all compositions was the mobility of a mixture of cement–sand mortar, characterized by a cone spread of 106–108 mm. Mobility was determined according to GOST 310.4-81 [52]. Based on the test results, the water-binding ratio (W/B) was adjusted until the required mobility parameters were achieved. In addition, for all compositions, the start and end dates of setting were determined in accordance with GOST 30744-2001 [51].

The study of the structure of cupola dust included experiments to determine the particle size distribution and assess the fineness of grinding during mechanical activation and chemical analysis of the oxide composition. The granulometric composition of the cupola dust was carried out using the sieve method without washing, according to GOST 12536-2014 [53].

Mechanical activation or grinding was carried out on raw materials from cupola dust that passed through 0.16 mm and 0.63 mm sieves. This work was carried out using a laboratory ball mill consisting of steel balls. The grinding fineness of cupola dust was determined by the gas permeability method of Kozeny and Karman using the PSH-12 device. Specific surface area (cm²/g) and mass average particle size (μm) were taken as the main parameters. The true density of the cupola dust was determined in accordance with GOST 30744-2001 [51] using the Le Chatelier instrument, with dehydrated kerosene as a liquid to prevent the formation of hydrate phases in the instrument, leading to distortion of the results. The mass of samples was measured on a VK-300 analytical balance with an accuracy of 0.01 g.

To study the properties and features of the structure formation of the studied compositions, control samples of 40 × 40 × 160 mm in size were taken in accordance with GOST 30744-2001 [51].

In the manufacture of control samples, a mode based on the recommendations for slag-alkali cements given in work [15], as well as the requirements for a standard cement mortar GOST 30744-2001 [51], were developed. The sequence and duration of operations for standard Portland cement and compositions of alkali-activated binders are given in Table 4.

Table 4. Technological regime for making and storing test samples.

Stage	Name of Process Operation	Process Characteristic	Operation Duration		
			Unit	Portland Cement	Alkali-Activated Binder
1	Binder and lye (water) dosage	Binder is added to the propeller stirrer and lye (water) is poured in.	s	30	30
2	Activation of the binder with alkali (water)	Mixing the binder with lye (water), low paddle speed	s	30	120 ¹
3	Dosage of fine aggregate (sand)	Fine aggregate (sand) is added to the propeller mixer	s	30	30 ¹
4	Mixing the mortar	Mixing sand with activated binder, high paddle speed	s	150	150 ¹
5	Gaining strength under temperature and humidity conditions	Pre-exposure of samples at normal room conditions	d	–	1
		In a 3 + 6 + 3-h temperature and humidity chamber.	h	12	12
	Gaining strength in the natural curing chamber	Pre-exposure of samples at normal room conditions	d	–	3
		Storage in a natural curing chamber with an odour trap	d	28	25

¹ Total stirring time (steps 2, 3, 4) according to [15], not more than 5 min or 300 s.

To assess the physical and mechanical properties of the samples, the following main indicators were taken: the bending strength of the beams and the compressive strength of the halves of these samples. Determination of the compressive strength of samples of natural hardening was being carried out for 3, 7 and 28 days by a non-destructive control method using the ONIKS device. Determination of the flexural and compressive strength by the destructive method was carried out using a PGM-500MG4 hydraulic press according to GOST 30744-2001 [51] within the following period: for samples of natural hardening—28 days; for samples subjected to temperature and humidity treatment, the test time was taken to be 2 h after removal from the chamber.

The average density of the samples after hardening was determined according to GOST 12730.1-2020 [54] at normal humidity, i.e., when the specimens are removed from a sealed accelerated curing chamber in which the relative humidity of the air is not less than 95% and the temperature is $(20 \pm 2)^\circ\text{C}$. The evaluation of the structure of the cement matrix of the obtained samples was evaluated in accordance with GOST 12730.4-2020 [55] according to the following indicators: average density (kg/m^3), true density (g/cm^3), water absorption by mass (%), relative density and material porosity.

X-ray phase analysis consisted in carrying out a qualitative assessment of the mineralogical composition of the diffraction patterns of cupola dust and cement stone of compositions C4, C6 and C7, as well as in determining the degree of crystallinity of the cupola dust. X-ray diffraction patterns were recorded with the help of a D2 Phaser diffractometer in the angle range of $10\text{--}70^\circ$ at a rate of 0.02° . The diffraction patterns were interpreted using the Match! program and the IDDC PDF+ database. The degree of crystallinity of cupola dust was determined with the TOPAS.Bruker program. The chemical composition of the

cupola dust was measured using an energy-dispersive X-ray fluorescence spectrometer, EDX-800 HS.

3. Results

3.1. Results of a Study on the Structure of Cupola Dust

The granulometric composition of cupola dust without preparation is shown in Figure 2.

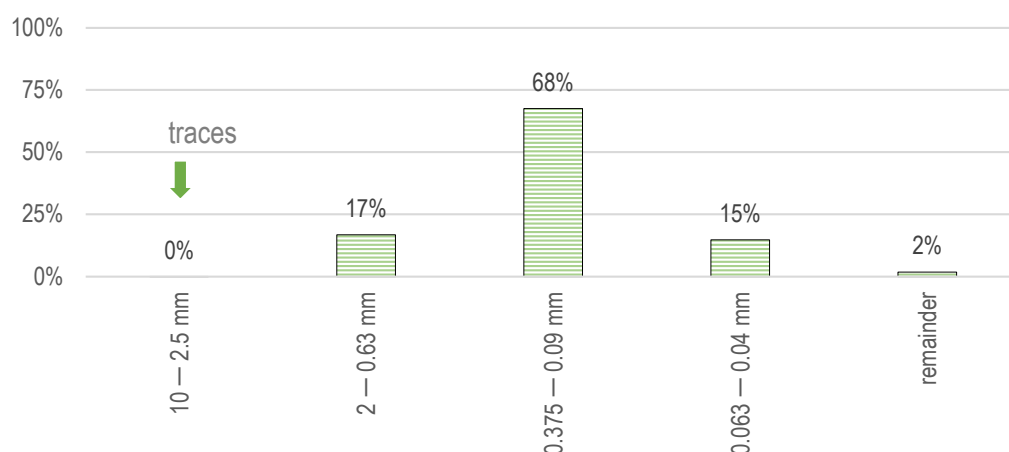


Figure 2. The particle size distribution of cupola dust.

There is a small number of large inclusions larger than 2.5 mm. The largest amount of cupola dust residue is in the range of 0.09–0.375 mm. It should be noted that for Portland cement, the control indicator is a sieve of 0.09 mm, the residue on which should be 1%, according to [56]. Obviously, the preparation of raw materials is required, namely, the grinding of fractions larger than 0.09 mm. However, for this type of raw material, due to the large amount of residue of 85% on sieves more than 0.09 mm, the researchers decided to screen the cupola dust through 0.63 mm and 0.16 mm sieves, followed by mechanical activation to change the grinding fineness.

The results of the study of fineness of grinding are shown in Table 5.

Table 5. Variation in the grinding fineness of cupola dust as a function of mechanical activation time.

Size of Test Sieve for Sieving Raw Materials, mm	Grinding Time, s	Specific Surface Area, m ² /kg	Mass Average Particle Size, μm
0.16	0	429	5.5
	60	605	3.9
	120	733	3.2
	240	771	3.1
0.63	0	265	8.9
	60	349	6.8
	120	384	6.1
	240	442	5.8

Four cases of using cupola dust were taken for further research: sifting through a 0.16 mm sieve, grinding for 60 s, dust passing through a 0.16 mm sieve, grinding for 120 s, dust passing through a 0.16 mm sieve, grinding for 240 s and dust passed through a 0.16 mm sieve. With prolonged grinding for more than 120 s, cementation of the mill walls with grinding products is noted.

The results of chemical analysis of the content of basic oxides in cupola dust are shown in Table 6.

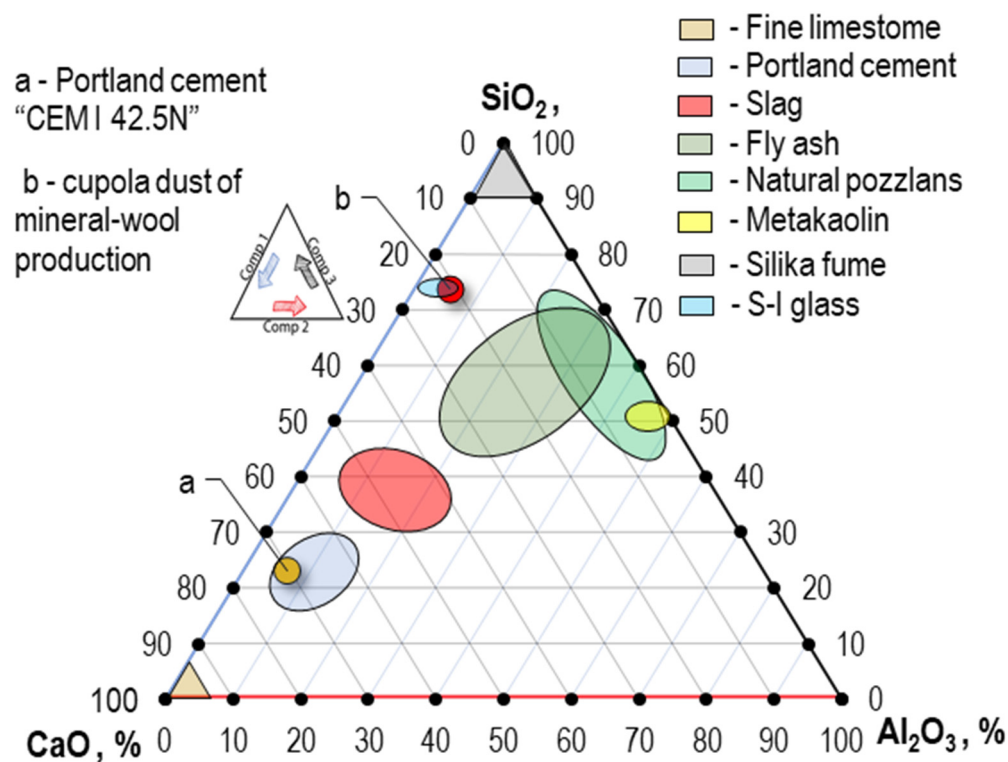
Table 6. Chemical composition of cupola dust.

$\text{Fe}_2\text{O}_3 + \text{FeO}$	Al_2O_3	SiO_2	CaO	MgO	TiO_2	ZnO	SO_3	$\text{Na}_2\text{O} + \text{K}_2\text{O}$	Loss on Ignition
7.38	3.56	53.18	14.82	9.90	0.18	1.39	1.64	7.65	25.76
	4.97	74.31	20.70	← The percentage of basic oxides reduced to 100% of the $\text{CaO}-\text{Al}_2\text{O}_3-\text{SiO}_2$ system					

The chemical composition of cupola dust showed the presence of a large amount of SiO_2 . The dust is not silica fume or fly ash and tends to the glass area. The basicity modulus is $M_k = 0.44$ —the dust belongs to the low basic ones.

Obviously, when a traditional binder (Portland cement) is used in mortars and concretes together with this raw material, the latter will be an inert mineral additive. From the standpoint of an alkali-activated binder, it is one of the promising raw materials.

Figure 3 shows a three-axis diagram of the $\text{CaO}-\text{SiO}_2-\text{Al}_2\text{O}_3$ system, indicating the points characteristic of Portland cement grade CEM I 42.5N and cupola dust. As the initial data for constructing this diagram, the data of the study of the phase transformation during alkaline activation were taken, in which a three-axis diagram is shown, indicating the raw materials in the $\text{CaO}-\text{SiO}_2-\text{Al}_2\text{O}_3$ system [57].

**Figure 3.** Three-axis diagram of the $\text{CaO}-\text{SiO}_2-\text{Al}_2\text{O}_3$ system.

When considering the $\text{CaO}-\text{SiO}_2-\text{Al}_2\text{O}_3$ system, cupola dust enters the zone tending to pure quartz or microsilica and is also located next to the glass zone, which makes it possible to obtain an alkali-activated binder.

The diffraction pattern of cupola dust with the results of a qualitative X-ray phase analysis is in Figure 4.

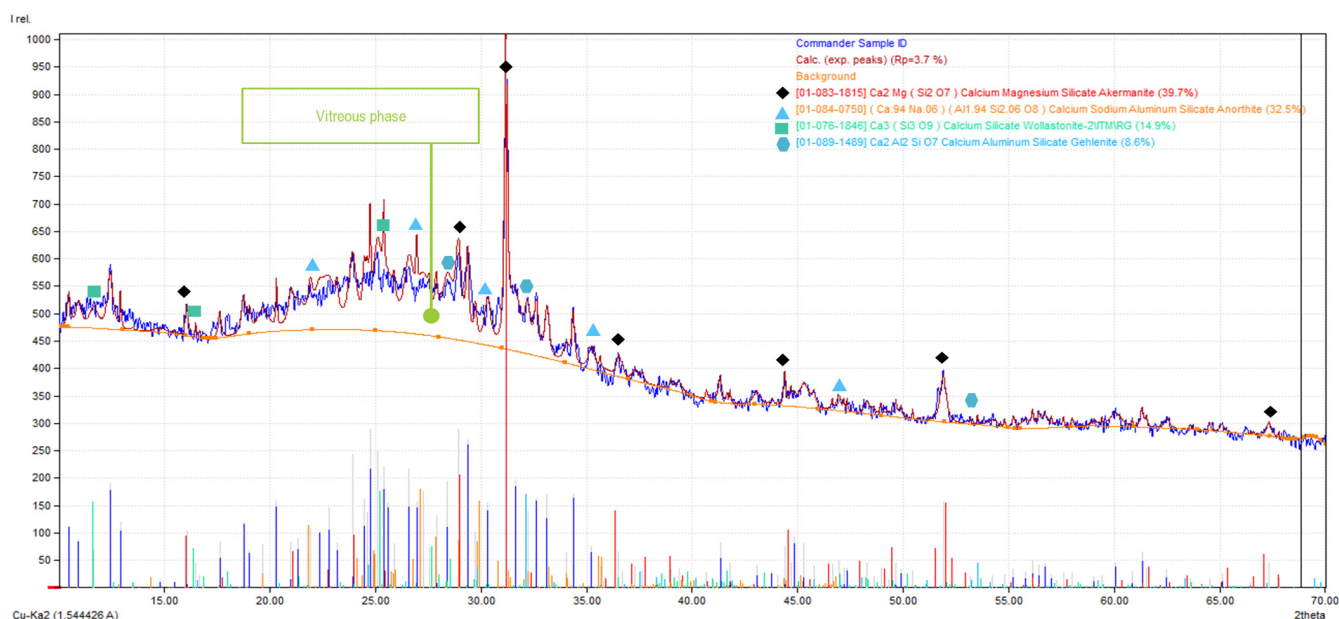


Figure 4. Diffractogram of cupola dust from mineral wool production.

The diffraction pattern clearly shows two halos in the range of double angles of $10\text{--}16^\circ$ (partially) and $17\text{--}36^\circ$. This indicates the presence of an amorphous phase. In addition, the presence of peaks in the diffraction pattern indicates the presence of crystalline phases, which are apparently subjected to partial melt, which is confirmed by the results of the melting of basalt [58].

The calculation of the degree of crystallinity of the dust showed that the crystalline phases make up 36.96% of the total sample volume and the amorphous phases, 63.04%. Based on this, it can be concluded that the structure of cupola dust includes glassy structures that contribute to additional hydration in alkaline conditions. According to the results of qualitative X-ray phase analysis, the presence of akermanite $\text{Ca}_2\text{MgSi}_2\text{O}_7$, gehlenite $\text{Ca}_2\text{Al}_2\text{SiO}_7$ in cupola dust, caused by the action of aluminosilicate melts on minerals of the gabbro-basalt group of plagioclases in the form of anorthite $\text{CaAl}_2\text{Si}_2\text{O}_8$, was established. The presence of wollastonite-2M $\text{Ca}_3(\text{Si}_3\text{O}_9)$ in the dust is possible.

3.2. Results of Research into the Influence of Technological Parameters on the Properties of Alkali Activated Binders Made from Cupola Dust

The results of technological parameters of mortar mixtures showed the following. When mixing cupola dust and sand with an alkaline activator, its increased amount is required in comparison with the use of Portland cement. The cone spread for all compositions corresponded to the range of 106–108 mm. The beginning of the setting time of the solution for composition C1 is 170 min and for compositions C2, C3, C4 and C5, 190–195 min. The end of the setting time for C1 is 260 min and for C2, C3, C4 and C5, more than 480 min. It should be noted that the composition C4 130 min after alkaline activation had the effect of false setting of the cement stone.

The visual assessment of the composition showed that the surface structure of the samples as a whole has a dense structure. However, composition C2 has deep cavities. Examples of samples of the composition C1, C2 and C3 are shown in Figure 5.

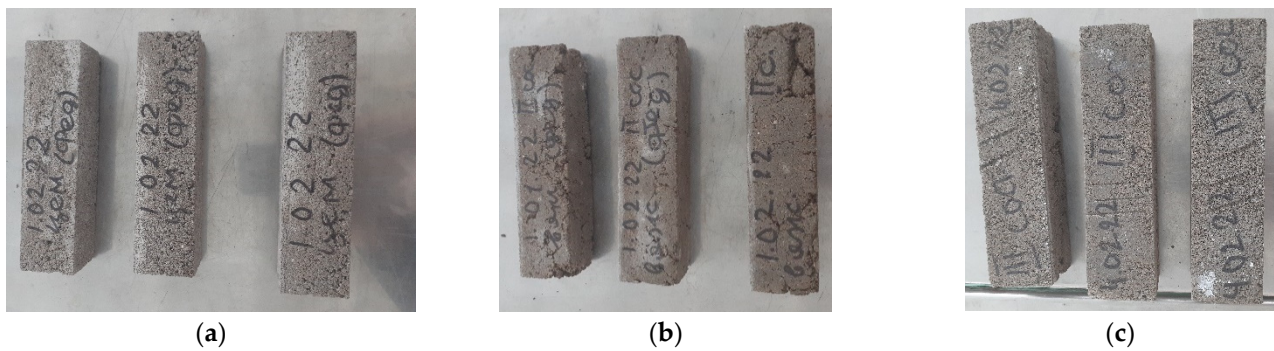


Figure 5. General view of the samples: (a) C1a composition, (b) C2a composition, (c) C3a composition.

Curves of the kinetics of hardening compositions C1a, C2a, C3a, C4a and C5a, obtained from the results of non-destructive testing of compressive strength, are shown in Figure 6.

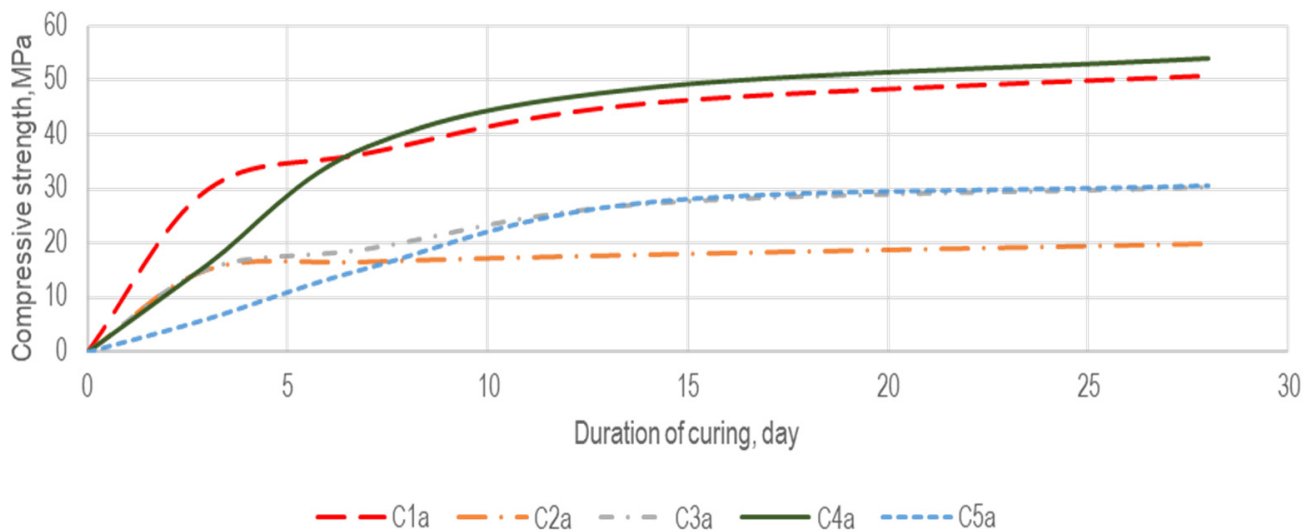


Figure 6. Gaining strength kinetics of C1a, C2a, C3a, C4a and C5a control formulations.

The nature of the strength development of C4a generally corresponds to the reference composition C1a. However, this composition is characterized by a rapid set of strength in the first two days. In turn, the low strength development of alkali-activated binders in the initial period is obviously caused by hardening in the open air in the first three days. C4a showed the highest strength with a characteristic mechanical activation of 120 s. Cupola dust with mechanical activation of 120 s was adopted for further research.

The results of testing the bending strength of the compositions under consideration after 28 days of natural hardening and hardening in the temperature–humidity treatment chamber are shown in Figure 7.

Composition C6 has the highest flexural and compressive strength under different hardening conditions. The lowest bending and compressive strength was shown by the composition C2, the highest, C6. The difference in strength in 28 days of hardening between the reference compositions C1 and C6 was 65% in bending and 33% in compression. The difference in strength readings between compositions with different alkaline activators C4 and C7 in 28 days of hardening showed almost the same result, 15% for bending strength and 2% for compression.

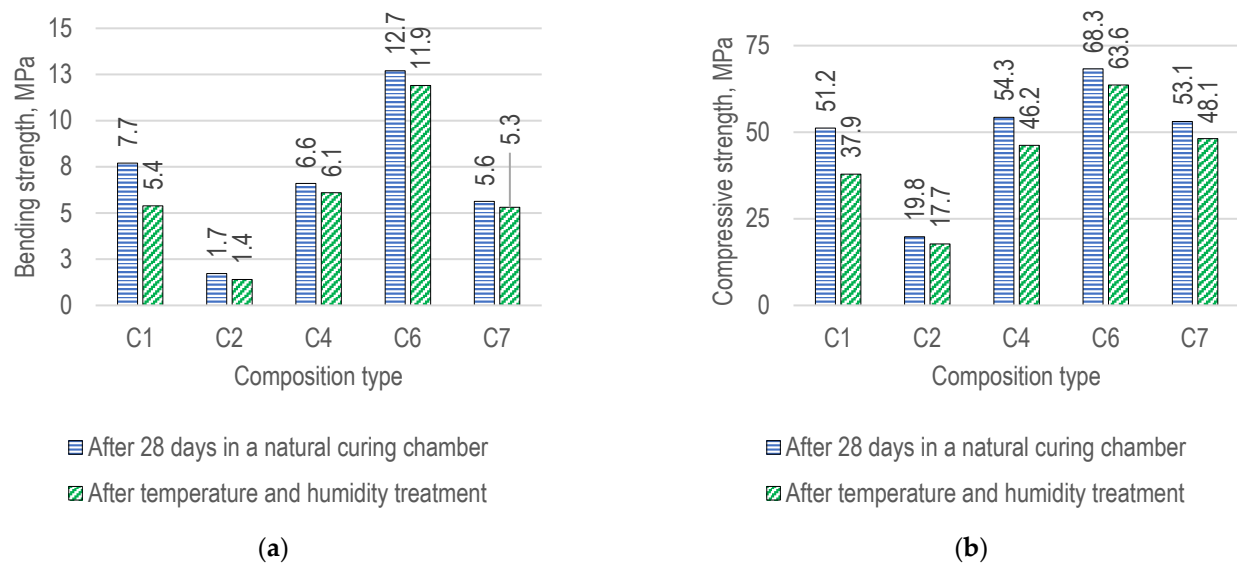


Figure 7. Test results of the specimens: (a) bending strength of the bars; (b) compression strength of the bar halves.

When considering the influence of hardening conditions, the results of the study showed that the percentage difference in bending strength during temperature–humidity treatment for the reference composition C1 is 70% of the strength value in 28 days of hardening. For samples from compositions C2, C4, C6 and C7, the average value of the bending strength is 90% and the compressive strength is 90%. The smallest set of strength was shown by the C2 composition in bending—81%.

3.3. Results of a Study of the Structure of an Alkali Activated Cement Matrix

The main indicators of the formed structure of the samples based on the alkali-activated binder compositions C4b, C6b and C7b are shown in Table 7.

Table 7. Density and porosity values of samples from compositions C4b, C6b and C7b.

Indicator	Composition Number		
	C4b	C6b	C7b
Average density normal humidity state, kg/m ³	2121	2130	2179
True density, kg/cm ³	2820	2790	2830
Water absorption by mass, %	8.1	6.1	8.1
Relative density	0.75	0.76	0.76
Material porosity, %	25	24	24

The difference in the degree of water absorption by the weight of the samples was established. Thus, the lowest water absorption is in the composition C6b; in turn, in the compositions C4b and C7b, the values are the same. The average, true density, relative density and porosity of the sample material are practically the same.

The results of a qualitative X-ray phase analysis of samples from the compositions C4b, C6b and C7b are shown in Figure 8.

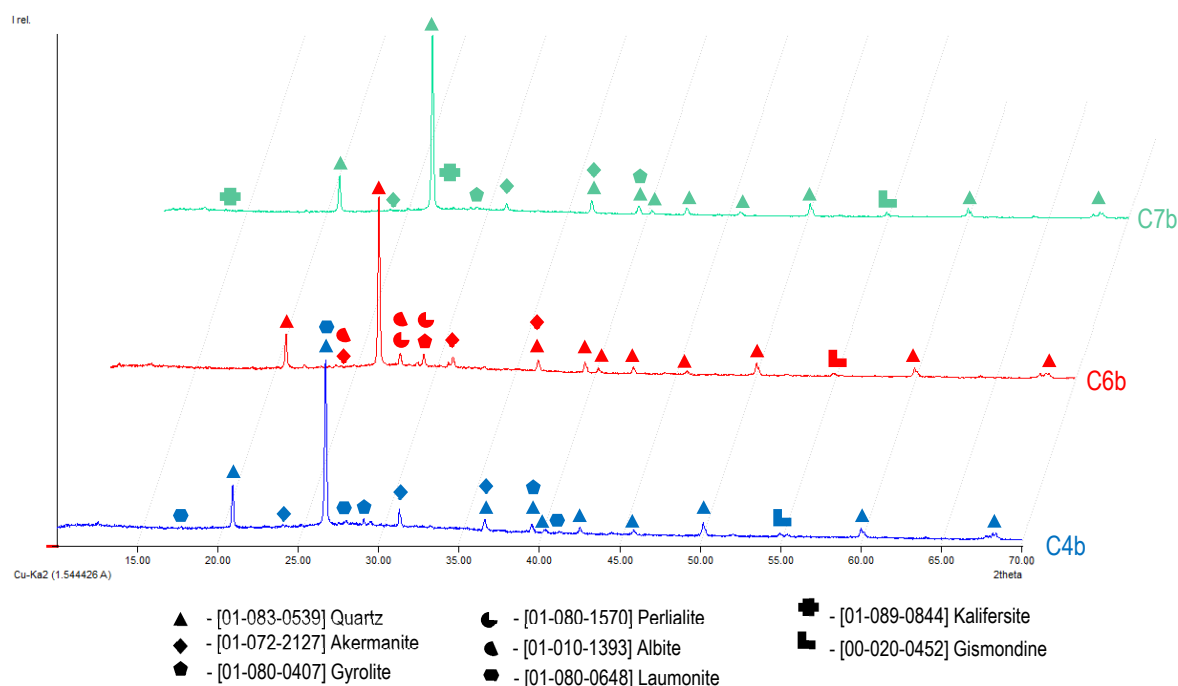


Figure 8. Diffractograms of cement–sand mortar samples using compositions C4b, C6b and C7b.

A comparative analysis of the diffraction patterns showed the presence of a distinctive area in the range from 27 to 32°. There is a halo of the amorphous phase in the range of 20 to 40°.

All diffraction patterns show pronounced peaks of quartz SiO_2 . The presence of akermanite $\text{Ca}_2\text{MgSi}_2\text{O}_7$ as a non-hydrated mineral of cupola dust is also noted.

The end products of hardening of binders based on cupola dust and its alkaline activation are low-basic calcium hydrosilicates of the calcium zeolite type gismondine $\text{Ca}_2\text{Al}_4\text{Si}_4\text{O}_{16} \cdot 9(\text{H}_2\text{O})$, as well as hydroaluminosilicates of the gyrolite type $\text{NaCa}_{16}\text{Si}_{23}\text{AlO}_{60}(\text{OH})_8 \cdot 14\text{H}_2\text{O}$, as a product of hydration under temperature and humidity conditions, which are characteristic of slag binders' processing. It is also possible that C4b contains laumonite $\text{Ca}(\text{Si}_4\text{Al}_2)\text{O}_{12} \cdot 4\text{H}_2\text{O}$, belonging to the zeolite group, C6b contains perialite $\text{K}_9\text{NaCa}(\text{Si}_{24}\text{Al}_{12})\text{O}_{72} \cdot 15\text{H}_2\text{O}$, which belongs to the zeolite group, and C7b contains kalifersite $(\text{K},\text{Na})_5\text{Fe}^{3+}_7\text{Si}_{20}\text{O}_{50}(\text{OH})_6 \cdot 12\text{H}_2\text{O}$, that belongs to the group of palygorskites.

Considering the mineralogical composition of the hardening products as a whole, we can conclude that the main minerals of the cement matrix are zeolites, which is in good agreement with the results given in [16].

4. Discussion

The results of theoretical and experimental studies generally show the possibility of using cupola dust of mineral wool production as the main raw material for an alkali-activated binder with obtained physical and mechanical properties characteristic of Portland cement.

When using the actual granulometric composition without preparation of raw materials, a significant decrease in strength is noted due to the low intensity of hydration processes that form the cement matrix. The need for additional grinding is also noted in [17]. It is possible that it is rational to adhere to the known limits of fineness of grinding in the production of a binder from dust, to carry out sifting through a 0.016 sieve, followed by mechanical activation for 120 s. With prolonged grinding of dust, a cemented crust is formed on the walls of the mill, which is a defect in the grinding process. In the future, it will be necessary to develop a technological mode of grinding which allows us to obtain the raw materials of the proper fineness of grinding with fewer losses. There is also an alternative method, such as the joint grinding of dust and mineral additives [59], which

helps to reduce the harmful factor. This method requires additional verification due to the changing composition affecting the properties and structure of the cement matrix.

The increase in the strength of concrete on the 28th day of hardening after grinding by 60, 120 and 240 sec. cupola dust is explained by an increase in the degree of the chemically active state of the particles, namely due to the activation of dust minerals in an alkaline solution with the formation of mineral nanosized particles (3.1–3.9 μm), which are additional centers of crystallization during the formation of the structure of the cement matrix. Similar processes were observed in the study of Portland cement with varying degrees of specific surface [60], as well as alkali-activated binders based on slag and fly ash [43]. A slight decrease in strength after mechanical activation for 240 s is possibly due to an alkaline activator deficiency caused by a greater degree of water demand. This, in turn, led to a decrease in the formation of hydration products.

The acceleration of hardening as a result of isothermal heating of the samples showed a generally positive result and confirmed that there was an increase in the degree of chemical interaction between cupola dust particles and an alkaline activator. Similar results were obtained in works [45,46].

The presence of an amorphous phase in cupola dust indicates the possible presence of aluminosilicate glassy elements. They contribute to a deeper and more intensive process of hydration of the binder during alkaline activation. As a result, more N-A-S-H gel is formed, which is responsible for the strength of the cement matrix. Similar results were obtained in works [35,61].

When using a solution of the composition of 50 wt.% caustic soda and 50 wt.% liquid glass as an activator, the maximum results of mechanical strength are obtained. The rheological properties of the mixture and the packing density of the cement matrix are improved. The introduction of Na_2SiO_3 promotes the formation of long-chain silicate oligomers, which, in turn, contribute to the intensive formation of N-A-S-H, increasing the strength of the cement matrix. In addition, Na_2SiO_3 is an additional reserve of silica in the binder. These results generally agree with the results [62] obtained with alkaline activation of fly ash with a CaO content of 16.6%.

The results are in good agreement with the comparative analysis of a mixture of Portland cement and slag binders described in [42]. However, due to the peculiarities of the production of liquid glass, there are factors that contribute to the pollution of the environment [63]. In the future, it is necessary to look for ways to reduce the use of liquid glass by replacing it with chemical additives.

Having considered the obtained results, it can be assumed that a binder based on cupola dust of mineral wool production may well be suitable as a component of a repair or concrete mixture for concrete and reinforced concrete, with appropriate optimization of the compositions.

In the future, the authors of this study plan to carry out a series of works on modifying the obtained compositions by adding various mineral and chemical additives to regulate the physical, mechanical and technological properties of concrete, such as hardening time, reducing the water-binding ratio. The key issue remains the decrease in the amount of liquid glass in the alkaline activator.

A separate direction in the development of this research is the study of the durability of alkali-activated concretes based on cupola dust from the standpoint of frost resistance and resistance in gas and liquid media.

5. Conclusions

Based on the results of the research, the following conclusions can be drawn:

- Analysis of the structure of cupola dust of mineral wool production allowed us to establish its suitability as a raw material for the production of alkali-activated binder with appropriate technological preparation: screening through a 0.16 mm sieve and mechanical activation 120 s to a specific surface area of $733 \text{ m}^2/\text{kg}$.

- It was experimentally established that the composition of cupola dust with an alkaline activator is 50 wt.% NaOH concentration 8.3 M and 50 wt.% Na_2SiO_3 showed the best results. The maximum bending strength in 28 days is 12.7 MPa; in compression, it is 68.3 MPa. The use of temperature and humidity treatment of samples from a cement–sand mortar together with an alkali-activated binder accelerates strength gain. At the same time, the difference between the strength values of natural hardening conditions for 28 days is no more than 20%.
- The mineralogical composition of the products of the structure formation of the cement matrix from an alkali-activated binder based on cupola dust during temperature–humidity treatment has been clarified; namely, the presence of minerals of the zeolite group, such as gismondine and gyrolite, has been noted.

Author Contributions: Conceptualization, P.F. and D.S.; methodology, P.F.; investigation, D.S.; resources, P.F. and D.S.; data curation, D.S.; writing—original draft preparation, P.F.; writing—review and editing, P.F.; visualization, P.F.; supervision, D.S.; project administration, D.S. All authors have read and agreed to the published version of the manuscript.

Funding: This research was funded by the Ministry of Science and Higher Education of the Russian Federation within the framework of the Priority 2030 program. The topic of the research is SP4_TD_B6 “Development of low-carbon cement systems”.

Institutional Review Board Statement: Not applicable.

Informed Consent Statement: Not applicable.

Data Availability Statement: Not applicable.

Acknowledgments: The authors express their deep gratitude to the head of the laboratory of the department of building structures of the Ufa State Petroleum Technological University, G.Yu. Shagalin, and laboratory assistant G.F. Ishbuldina for conducting a number of studies, as well as to the staff of the Bashkir State University for conducting a chemical analysis of cupola dust.

Conflicts of Interest: The authors declare no conflict of interest. The funders had no role in the design of the study; in the collection, analyses or interpretation of data; in the writing of the manuscript or in the decision to publish the results.

References

1. Technical Report by the Bureau of the United Nations Statistical Commission (UNSC) on the Process of the Development of an Indicator Framework for the Goals and Targets of the Post-2015 Development Agenda (Working Draft). Sustainable Development Knowledge Platform. United Nations 2015. Available online: [https://sustainabledevelopment.un.org/content/documents/6754Technical%20report%20of%20the%20UNSC%20Bureau%20\(final\).pdf](https://sustainabledevelopment.un.org/content/documents/6754Technical%20report%20of%20the%20UNSC%20Bureau%20(final).pdf) (accessed on 3 August 2022).
2. Zhang, C.-Y.; Han, R.; Yu, B.; Wei, Y.-M. Accounting Process-Related CO₂ Emissions from Global Cement Production under Shared Socioeconomic Pathways. *J. Clean. Prod.* **2018**, *184*, 451–465. [CrossRef]
3. Cement Production Global. 2021. Available online: <https://www.statista.com/statistics/1087115/global-cement-production-volume/#statisticContainer> (accessed on 3 August 2022).
4. Geological Survey. *Mineral Commodity Summaries 2022—Cement*; Geological Survey: Liston, VA, USA, 2022.
5. Wu, T.; Ng, S.T.; Chen, J. Deciphering the CO₂ Emissions and Emission Intensity of Cement Sector in China through Decomposition Analysis. *J. Clean. Prod.* **2022**, *352*, 131627. [CrossRef]
6. Vasilik, G.Y.; Eremina, Y.M. Russian cement industry in 2020. *J. Cem. Its Appl.* **2020**, *6*, 22–33.
7. *Technology Roadmap Low-Carbon Transition in the Cement Industry*; OECD/International Energy Agency: Paris, France, 2018.
8. International Energy Agency (IEA). *Energy Technology Perspectives*. In *Scenarios & Strategies to 2050*, 1st ed.; IEA/OECD: Paris, France, 2006.
9. Brice, D.G.; Ko, L.S.-C.; Provis, J.L.; van Deventer, J.S.J. Conclusions and the Future of Alkali Activation Technology. In *Alkali Activated Materials*; Provis, J.L., van Deventer, J.S.J., Eds.; RILEM State-of-the-Art Reports; Springer: Dordrecht, The Netherlands, 2014; Volume 13, pp. 381–388. ISBN 978-94-007-7671-5.
10. Richardson, I.; Taylor, H.F.W. *Cement Chemistry*; ICE Publishing Institution of Civil Engineers: London, UK, 2013; ISBN 978-0-7277-4179-0.
11. Shepelenko, T.S.; Zubkova, O.A.; Subbotina, N.V.; Luchnikova, E.E.; Zykeev, G.A. Composite Cements Containing Sucrose. *Vestnik TGASU* **2017**, *5*, 151–158.
12. Kaminskas, R.; Kubiliute, R. Artificial Pozzolana from Silica Gel Waste–Clay–Limestone Composite. *Adv. Cem. Res.* **2014**, *26*, 155–168. [CrossRef]

13. Schneider, M. The Cement Industry on the Way to a Low-Carbon Future. *Cem. Concr. Res.* **2019**, *124*, 105792. [CrossRef]
14. Zajceva, L.; Lucyk, E.; Latypova, T.; Latypov, V.; Fedorov, P.; Salamanova, M. Influence of the Type of Aggregate from Industrial Waste on Corrosion Resistance of Modified Fine-Grained Concrete. *Buildings* **2021**, *11*, 352. [CrossRef]
15. Gluhovskij, V.D.; Pahomov, V.A. *Slag-Alkali Cements and Concretes*; Budivel'nik: Kyiv, Ukraine, 1978.
16. Davidovits, J. *Geopolymer: Chemistry and Applications*, 5th ed.; Institut Géopolymère: Saint-Quentin, France, 2020; ISBN 978-2-9544531-1-8.
17. Erofeev, V.; Rodin, A.; Yakunin, V.; Bogatov, A.; Bochkin, V.; Chegodaikin, A. Alkali-Activated Slag Binders from Rock-Wool Production Wastes. *Mag. Civ. Eng.* **2018**, *6*, 219–227. [CrossRef]
18. Rusina, V.V. Ash Slag-Alkaline Binders Based on Liquid Glass from Impurities Containing Microsilica. *Stroit. Mater.* **2011**, *11*, 25–29.
19. Palomo, A.; Palacios, M. Alkali-Activated Cementitious Materials: Alternative Matrices for the Immobilisation of Hazardous Wastes. *Cem. Concr. Res.* **2003**, *33*, 289–295. [CrossRef]
20. Papadakis, V.G. *Estimation of Concrete Service Life—The Theoretical Background*, 1st ed.; Patras Science Park SA: Patras, Greece, 2005.
21. Alekseev, S.N.; Rosenthal, N.K. *Corrosion Resistance of Reinforced Concrete Structures in Aggressive Industrial Environment*; Stroyizdat: Moscow, Russia, 1976.
22. Latypov, V.M.; Latypova, T.V.; Lutsyk, E.V.; Fedorov, P.A. *Durability of Concrete and Reinforced Concrete in Natural Aggressive Environments*, 2nd ed.; USPTU Editorial and Publishing Center: Ufa, Russia, 2014; ISBN 978-5-7831-1233-1.
23. Kramar, L.J.; Trofimov, B.J.; Chernyh, T.N.; Kirsanova, A.A.; Zimich, V.V. *Modifiers for Cement Concretes and Mortars Technical Characteristics and Mechanism of Action*; Publishing Center of SUSU: Chelyabinsk, Russia, 2017.
24. Kaprielov, S.S.; Shejnfel'd, A.V.; Kardumjan, G.S. *New Modified Concretes*; Tipografija Paradiz: Moscow, Russia, 2010.
25. Mehta, A.; Siddique, R. An Overview of Geopolymers Derived from Industrial By-Products. *Constr. Build. Mater.* **2016**, *127*, 183–198. [CrossRef]
26. Eroshkina, N.A.; Korovkin, M.O. *Geopolymer Building Materials Based on Industrial Waste*; Penza State University of Architecture and Construction: Penza, Russia, 2014.
27. Grass, K.; Bartashov, V.; Sucker, J. Recycling of Mineral Wool Waste. Available online: <https://www.ibe.at/wp-content/uploads/2021/03/Recycling-of-mineral-wool-waste-1.htm> (accessed on 3 August 2022).
28. Kizinievič, O.; Balkevičius, V.; Prancėvičienė, J.; Kizinievič, V. Investigation of the Usage of Centrifuging Waste of Mineral Wool Melt (CMWW), Contaminated with Phenol and Formaldehyde, in Manufacturing of Ceramic Products. *Waste Manag.* **2014**, *34*, 1488–1494. [CrossRef] [PubMed]
29. Official Publishing of the European Communities. *LIFE and Waste Recycling: Innovative Waste Management Options in Europe*; Schiessler, N., Kommission, E., Eds.; LIFE focus; Official Publishing of the European Communities: Luxembourg, 2007; ISBN 978-92-79-07397-7.
30. Stonys, R.; Kuznetsov, D.; Krasnikovs, A.; Škamat, J.; Baltakys, K.; Antonovič, V.; Černašėjus, O. Reuse of Ultrafine Mineral Wool Production Waste in the Manufacture of Refractory Concrete. *J. Environ. Manage.* **2016**, *176*, 149–156. [CrossRef] [PubMed]
31. Kubiliute, R.; Kaminskas, R.; Kazlauskaitė, A. Mineral Wool Production Waste as an Additive for Portland Cement. *Cem. Concr. Compos.* **2018**, *88*, 130–138. [CrossRef]
32. Nagrockienė, D. The Effect of Waste from Mineral Wool Manufacturing on the Properties of Concrete. *Ceram. Silik.* **2021**, *65*, 1–8. [CrossRef]
33. Belov, V.V.; Abramov, D.G. Evaluation of Mineral Wool Product Manufacturing Waste Effect on Mechanical Properties of Concrete. *Constr. Mater. Equip. Technol. XXI Century* **2019**, *5–6*, 33–36.
34. Kinnunen, P.; Yliniemi, J.; Talling, B.; Illiäinen, M. Rockwool Waste in Fly Ash Geopolymer Composites. *J. Mater. Cycles Waste Manag.* **2017**, *19*, 1220–1227. [CrossRef]
35. Puertas, F.; Torres-Carrasco, M. Use of Glass Waste as an Activator in the Preparation of Alkali-Activated Slag. Mechanical Strength and Paste Characterisation. *Cem. Concr. Res.* **2014**, *57*, 95–104. [CrossRef]
36. Granizo, M.L.; Alonso, S.; Blanco-Varela, M.T.; Palomo, A. Alkaline Activation of Metakaolin: Effect of Calcium Hydroxide in the Products of Reaction. *J. Am. Ceram. Soc.* **2004**, *85*, 225–231. [CrossRef]
37. Yip, C.K.; Lukey, G.C.; Provis, J.L.; van Deventer, J.S.J. Effect of Calcium Silicate Sources on Geopolymerisation. *Cem. Concr. Res.* **2008**, *38*, 554–564. [CrossRef]
38. Phoo-ngernkham, T.; Maegawa, A.; Mishima, N.; Hatanaka, S.; Chindaprasirt, P. Effects of Sodium Hydroxide and Sodium Silicate Solutions on Compressive and Shear Bond Strengths of FA–GBFS Geopolymer. *Constr. Build. Mater.* **2015**, *91*, 1–8. [CrossRef]
39. Phoo-ngernkham, T.; Hanjitsuwan, S.; Damrongwiriyanupap, N.; Chindaprasirt, P. Effect of Sodium Hydroxide and Sodium Silicate Solutions on Strengths of Alkali Activated High Calcium Fly Ash Containing Portland Cement. *KSCE J. Civ. Eng.* **2017**, *21*, 2202–2210. [CrossRef]
40. Sajedi, F.; Razak, H.A. The Effect of Chemical Activators on Early Strength of Ordinary Portland Cement-Slag Mortars. *Constr. Build. Mater.* **2010**, *24*, 1944–1951. [CrossRef]
41. Palomo, A.; Grutzeck, M.W.; Blanco, M.T. Alkali-Activated Fly Ashes. *Cem. Concr. Res.* **1999**, *29*, 1323–1329. [CrossRef]
42. Ruengsillapanun, K.; Udtaranakron, T.; Pulngern, T.; Tangchirapat, W.; Jaturapitakkul, C. Mechanical Properties, Shrinkage, and Heat Evolution of Alkali Activated Fly Ash Concrete. *Constr. Build. Mater.* **2021**, *299*, 123954. [CrossRef]

43. Karim, M.R.; Hossain, M.M.; Manjur, A.; Elahi, M.; Zain, M.F.M. Effects of Source Materials, Fineness and Curing Methods on the Strength Development of Alkali-Activated Binder. *J. Build. Eng.* **2020**, *29*, 101147. [[CrossRef](#)]
44. Rybak, J.; Kongar-Syuryun, C.; Tyulyaeva, Y.; Khayrutdinov, A.M. Creation of Backfill Materials Based on Industrial Waste. *Minerals* **2021**, *11*, 739. [[CrossRef](#)]
45. Castillo, H.; Collado, H.; Droguett, T.; Sánchez, S.; Vesely, M.; Garrido, P.; Palma, S. Factors Affecting the Compressive Strength of Geopolymers: A Review. *Minerals* **2021**, *11*, 1317. [[CrossRef](#)]
46. Adam, A.A.; Horiato, X.X.X. The Effect of Temperature and Duration of Curing on the Strength of Fly Ash Based Geopolymer Mortar. *Procedia Eng.* **2014**, *95*, 410–414. [[CrossRef](#)]
47. Ermolovich, E.A.; Ivannikov, A.L.; Khayrutdinov, M.M.; Kongar-Syuryun, C.B.; Tyulyaeva, Y.S. Creation of a Nanomodified Backfill Based on the Waste from Enrichment of Water-Soluble Ores. *Materials* **2022**, *15*, 3689. [[CrossRef](#)]
48. Wang, A.; Zheng, Y.; Zhang, Z.; Liu, K.; Li, Y.; Shi, L.; Sun, D. The Durability of Alkali-Activated Materials in Comparison with Ordinary Portland Cements and Concretes: A Review. *Engineering* **2020**, *6*, 695–706. [[CrossRef](#)]
49. Wardhono, A.; Law, D.W.; Molyneaux, T.C.K. Long Term Performance of Alkali Activated Slag Concrete. *J. Adv. Concr. Technol.* **2015**, *13*, 187–192. [[CrossRef](#)]
50. GOST 23732-2011; Water for Concrete and Mortars. Specifications. Standartinform: Moscow, Russia, 2012.
51. GOST 30744-2001; Cements. Methods of Testing with Using Polyfraction Standard Sand. Gosstroy of Russia: Moscow, Russia, 2001.
52. GOST 310.4-81; Cements. Methods of Bending and Compression Strength Determination. IPK Izdatel'stvo standartov: Moscow, Russia, 2003.
53. GOST 12536-2014; Soils. Methods of Laboratory Granulometric (Grain-Size) and Microaggregate Distribution. Standartinform: Moscow, Russia, 2019.
54. GOST 12730.1-2020; Concretes. Methods of Determination of Density. Standartinform: Moscow, Russia, 2021.
55. GOST 12730.4-2020; Concretes. Methods of Determination of Porosity Parameters. Standartinform: Moscow, Russia, 2021.
56. GOST 310.2-76; Cements. Methods of Grinding Fineness Determination. IPK Izdatel'stvo standartov: Moscow, Russia, 2003.
57. Xiao, R.; Jiang, X.; Zhang, M.; Polaczyk, P.; Huang, B. Analytical Investigation of Phase Assemblages of Alkali-Activated Materials in CaO-SiO₂-Al₂O₃ Systems: The Management of Reaction Products and Designing of Precursors. *Mater. Des.* **2020**, *194*, 108975. [[CrossRef](#)]
58. Chen, X.; Zhang, Y.; Hui, D.; Chen, M.; Wu, Z. Study of Melting Properties of Basalt Based on Their Mineral Components. *Compos. Part B Eng.* **2017**, *116*, 53–60. [[CrossRef](#)]
59. Kravtsov, A.V.; Tsybakin, S.V. The Influence of Joint Grinding of Cement and Cooper Slag on Mortar Properties. *Vestn. MGSU* **2016**, *2016*, 64–77. [[CrossRef](#)]
60. Zhang, T.; Yu, Q.; Wei, J.; Zhang, P. Effects of Size Fraction on Composition and Fundamental Properties of Portland Cement. *Constr. Build. Mater.* **2011**, *25*, 3038–3043. [[CrossRef](#)]
61. He, P.; Zhang, B.; Lu, J.-X.; Poon, C.S. Reaction Mechanisms of Alkali-Activated Glass Powder-Ggbs-CAC Composites. *Cem. Concr. Compos.* **2021**, *122*, 104143. [[CrossRef](#)]
62. Chindaprasirt, P.; Chareerat, T.; Sirivivatnanon, V. Workability and Strength of Coarse High Calcium Fly Ash Geopolymer. *Cem. Concr. Compos.* **2007**, *29*, 224–229. [[CrossRef](#)]
63. Brykov, A.S. Production and Usage of Powdered Alkali Metal Silicate Hydrates. *Metallurgist* **2008**, *52*, 648–652. [[CrossRef](#)]